

## Review

## Dissecting deep brain stimulation evoked neural activity in the basal ganglia

M. Sohail Noor<sup>a</sup>, Alexandra K. Steina<sup>b</sup>, Cameron C. McIntyre<sup>a,c,\*</sup><sup>a</sup> Department of Biomedical Engineering, Duke University, Durham, NC, USA<sup>b</sup> Institute of Clinical Neuroscience and Medical Psychology, Heinrich Heine University, Düsseldorf, Germany<sup>c</sup> Department of Neurosurgery, Duke University, Durham, NC, USA

## ARTICLE INFO

## Keywords:

Subthalamic nucleus  
Globus pallidus  
Parkinson's disease  
Biomarker  
Evoked potential  
Oscillation  
Resonance  
Target engagement

## ABSTRACT

Deep brain stimulation (DBS) is an established therapeutic tool for the treatment of Parkinson's disease (PD). The mechanisms of DBS for PD are likely rooted in modulation of the subthalamo-pallidal network. However, it can be difficult to electrophysiologically interrogate that network in human patients. The recent identification of large amplitude evoked potential (EP) oscillations from DBS in the subthalamic nucleus (STN) or globus pallidus internus (GPI) are providing new scientific opportunities to expand understanding of human basal ganglia network activity. In turn, the goal of this review is to provide a summary of DBS-induced EPs in the basal ganglia and attempt to explain various components of the EP waveforms from their likely network origins. Our analyses suggest that DBS-induced antidromic activation of globus pallidus externus (GPe) is a key driver of these oscillatory EPs, independent of stimulation location (i.e. STN or GPI). This suggests a potentially more important role for GPe in the mechanisms of DBS for PD than typically assumed. And from a practical perspective, DBS EPs are poised to become clinically useful electrophysiological biomarker signals for verification of DBS target engagement.

## Introduction

High-frequency (>100 Hz) deep brain stimulation (DBS) applied within the subthalamic nucleus (STN) or the globus pallidus internus (GPI) are both effective treatments for the motor symptoms of late-stage Parkinson's disease (PD) [1]. Precise targeting of the motor subsections of the STN or GPI is considered crucial for therapeutic benefits from DBS [2, 3,4]. However, accurate electrode implantation can be challenging due to the small size of the nuclei. In turn, DBS surgeries are traditionally performed on awake patients, allowing the clinical team to evaluate electrophysiological recordings and behavioral responses to acute electrical stimulation for surgical target confirmation [5]. For example, intrinsic local field potentials (LFPs) within the beta frequency range (13–30 Hz), also known as beta oscillations, can exhibit unusually high power in PD patients [6,7]. This electrophysiological characteristic can aid in identifying the optimal stimulation contact for DBS therapy [8].

While awake electrophysiological recordings, from micro- and/or macro-electrodes, represent the traditional standard for target identification, recent trends in DBS surgical workflows are exploring opportunities to implant DBS electrodes with the patient under general anesthesia (GA) [9,10]. A key motivation for the use of asleep DBS

procedures is patient preference and their general comfort. However, challenges arise in asleep DBS due to the inability to measure behavioral responses to test stimulation pulses, as well as the suppression of intrinsic neural activity that can be caused by anesthesia [11]. In turn, substantial debate remains within the field on the pros and cons of awake vs. asleep surgical approaches.

One factor that could alleviate some of the reservations about employing asleep DBS surgical protocols would be the identification of a robust, reproducible, and accurate electrophysiological biomarker of DBS target engagement while patients are under GA. Along this line, recent advances in high-quality electrophysiology equipment and stimulation artifact removal techniques have enabled the recording of evoked potentials (EPs) in both the STN and GPI between and after DBS pulses [12,13,14]. Most of the analyses thus far have concentrated on STN EPs generated by STN DBS (Fig. 1). These STN EPs are not a stimulation artifact [13,18], and they have much larger amplitudes than intrinsic LFP signals (e.g. beta oscillations) [14].

Macro-electrode recordings from PD patients have demonstrated that STN EP amplitudes decrease as the recording electrode distance increases from the dorsolateral (i.e. motor) STN [14]. These signals are also not observed outside the STN when recording with micro-electrodes [17].

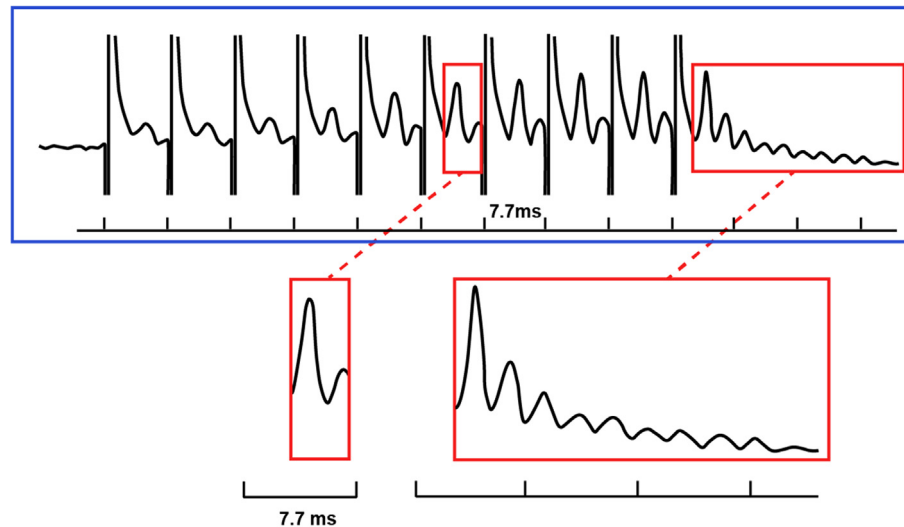
\* Corresponding author.

E-mail address: [cameron.mcintyre@duke.edu](mailto:cameron.mcintyre@duke.edu) (C.C. McIntyre).<https://doi.org/10.1016/j.neurot.2024.e00356>

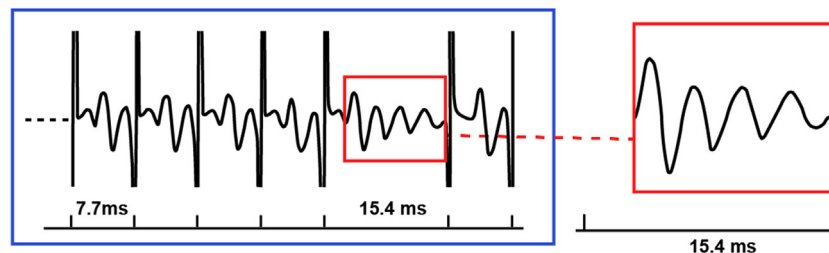
Received 15 November 2023; Received in revised form 26 March 2024; Accepted 1 April 2024

1878-7479/© 2024 The Author(s). Published by Elsevier Inc. on behalf of American Society for Experimental NeuroTherapeutics. This is an open access article under the CC BY-NC-ND license (<http://creativecommons.org/licenses/by-nc-nd/4.0/>).

### A. STN ERNA during and after a train of pulses at 130 Hz STN DBS



### B. STN ERNA when a pulse is skipped during 130 Hz STN DBS



### C. STN Evoke Recurrent Neural Activity during 20 Hz STN DBS

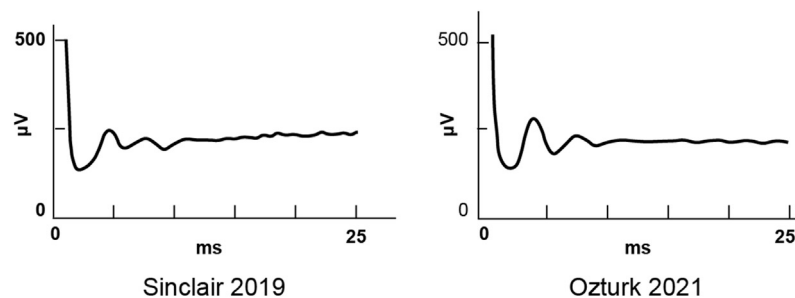


**Fig. 1.** Evoked Recurrent Neural Activity (ERNA) in the STN. Example signals recorded from the dorsal STN of PD patients. A) STN ERNA elicited during and after a train of 10 DBS pulses delivered to the STN at 130 Hz (Modified from Ref. [14]). B) STN ERNA elicited when one pulse was skipped during 130 Hz STN DBS (Modified from Ref. [15]). C) STN ERNA elicited during 20 Hz STN DBS (Left panel: modified from Ref. [16]; Right panel: modified from Ref. [17]).

Furthermore, they are not detected when stimulating and recording in the ventral intermediate nucleus of the thalamus of essential tremor patients [14]. However, similar DBS-induced EP waveforms have been recorded in the GPi of PD patients [12,13], as well as in the STN of dystonia patients [19,20]. These coupled observations suggests that these EP signals are explicitly associated with the subthalamo-pallidal circuit, but they are not necessarily associated with PD.

Unlike intrinsic LFP signals, DBS-induced EPs remain robustly detectable in patients under GA [14,21]. This underscores their potential significance for electrode targeting in the STN or GPi for either awake or anesthetized surgeries. Additionally, the change in the frequency of STN EPs correlates with the relative amplitude of beta oscillations [16], which is regarded as a biomarker for certain PD symptoms [6,7]. This suggests that besides serving as a potential biomarker for localizing the

stimulation target, DBS-induced EPs may also find useful applications as biomarker signals for closed-loop DBS systems designed to be triggered by the presence of symptoms.

The goal of this review is to provide a summary of DBS-induced EPs in the basal ganglia and attempt to explain the origins of various components of the EP waveforms. In general, these EPs consist of a strong decaying oscillation that is set in motion by the stimulus [22]. The EPs are comprised of multiple features that evolve over different time courses. They can be recorded after a single DBS pulse, during a train of pulses, or after the cessation of a train, and each situation exhibits interesting nuances that help expand understanding of the subthalamo-pallidal network. The oscillations are modulated by the complex interplay of excitatory and inhibitory synaptic connections that link the STN with the globus pallidus. Therefore, the goal of this report is

to work through the initial neural activation generated by a DBS pulse, and then follow the action potentials, conduction delays, and synaptic effects that underlie the ensuing oscillations.

Evoked Field Potentials

The basic biophysics of field potentials recorded by DBS electrodes are derived from the summation of transmembrane currents generated by the neural elements that surround the implanted lead [23]. These currents come from action potential signaling and synaptic communication, which subsequently create electric fields in the extracellular medium. When these electric fields overlap in time and space they can create a measurable signal that can be detected by either micro- or macro-electrodes [24]. Action potentials are of very short duration, and nearby neurons seldom fire with perfect synchrony, which is why their contribution to the extracellular field potential is typically limited. However, synaptic currents have slower dynamics that are more likely to overlap in time, and thus are typically the prime contributors to the field potential signals.

Inhibitory postsynaptic potentials (e.g. GABAergic synapses) yield positive deflections in the local extracellular environment [25,26]. They trigger an influx of predominately negative ions into the cells, inducing a positive field potential. Alternatively, excitatory postsynaptic potentials (e.g. glutamatergic synapses) result in negative deflections [26,27]. They trigger an influx of predominately positive ions into the cells, inducing a negative electric potential in the local extracellular environment. Interestingly, it should be noted that the polarity of these deflections for cortical recordings are typically reversed when analyzing signals from extra-cranial scalp electrodes [28].

The amplitude of intrinsic LFPs generated in the basal ganglia of PD patients (e.g. beta oscillations) typically fall within the microvolt range [29]. However, field potential amplitudes evoked by direct electrical stimulation are considerably larger and are typically in the millivolt range [13,14]. This is due to the enhanced neural synchronization induced by the stimulus. Large amplitude signals generally present an attractive feature for a biomarker, as signals with a high signal-to-noise ratio pose a less challenging engineering task for designing the recording circuitry. Thus, EPs can provide compelling benefits for use in clinical recording devices.

Evoked Potentials in the STN due to STN DBS

When a DBS pulse (or train of pulses) is delivered in the STN, a strong EP signal can be recorded [13,14] (Fig. 1). The EP signal is a decaying oscillation that has been set in motion by the stimulus. When a train of stimuli are used, the signal exhibits similar characteristics for either high or low frequency DBS. However, the decaying oscillation damps earlier when using lower frequency stimulation [17]. During a train of DBS pulses, the likely effects of synaptic plasticity can also be seen in the modulation of the EP signal over time [30]. For example, when the DBS pulse train is initiated, the amplitude of the initial EP waveform progressively increases, while its latency decreases, over the course of the first 10–20 DBS pulses. The evoked potential waveform then remains

stable over the next 100–200 DBS pulses. If the stimulation continues, the pattern reverses, with a slow decrease in the amplitude and increase in the latency, until the system finally reaches a steady state after ~80 s of DBS [13,15].

Standardizing Terminology

Various research groups have used different terms to describe these interesting EPs in the basal ganglia. Sinclair et al. initially coined the term “Evoked Resonant Neural Activity” (ERNA), noting its resemblance to a decaying oscillation [14,18] (Fig. 1). However, their characterization of this evoked response as “resonant” lacked substantiation since they did not conduct testing at other stimulation frequencies, which is crucial for discerning resonance. Subsequent research has shown that the amplitude of this evoked response does increase as the DBS frequency approaches 130 Hz and decreases at higher stimulation frequencies [13,15]. This suggests that an association between 130 Hz and the natural frequency of the circuit may exist, thereby supporting the concept of resonance within the circuit at ~130 Hz. For example, STN stimulation at lower frequencies also elicits an oscillatory evoked responses in the STN [13,16,17], but those responses are not technically resonant (Fig. 1c).

Comparison of ERNA characteristics to resonance in simple oscillatory systems, such as a simple pendulum, has led to conflict about the term ERNA. For example, oscillations in simple resonant systems typically reach a plateau at their peak amplitudes, while ERNA deviates by failing to maintain its peak amplitude, instead declining over time due to factors such as adaptation or short-term synaptic depression [31,15]. Furthermore, some researchers, noting changes in ERNA frequency after stimulation cessation, have suggested the absence of a natural frequency, and hence a lack of resonance [13]. These observations would hold true if damping were constant; however, the decrease in both ERNA amplitude and frequency suggests an increase in damping [32]. Additionally, since neural oscillators are typically not isolated but instead coupled with other oscillators [33], it is unlikely that their frequency would remain constant after stimulation cessation [34].

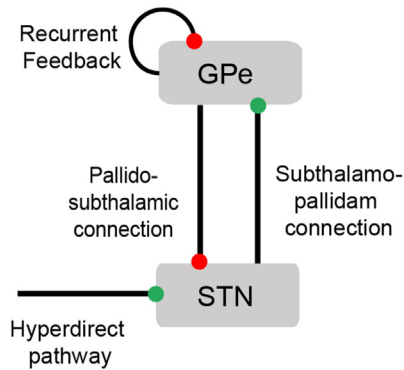
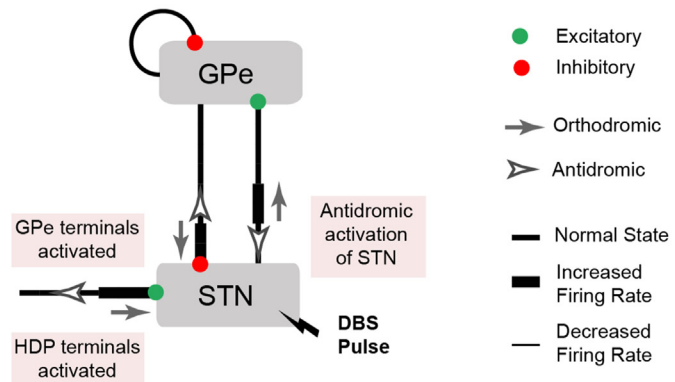
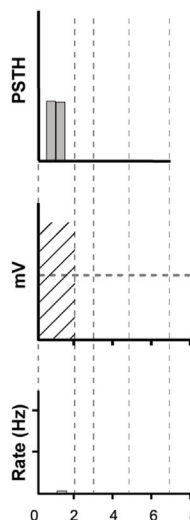
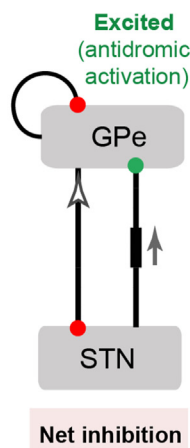
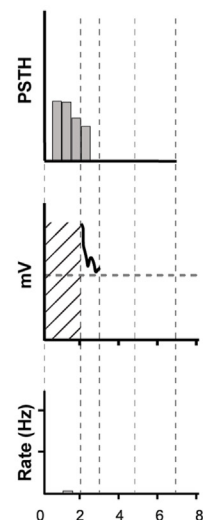
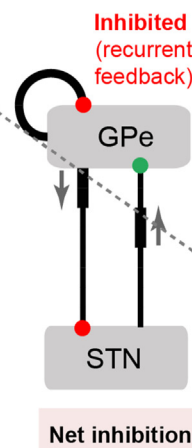
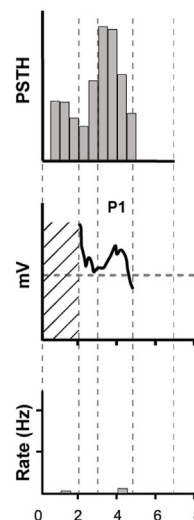
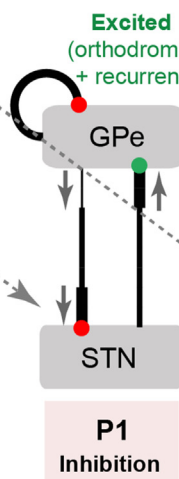
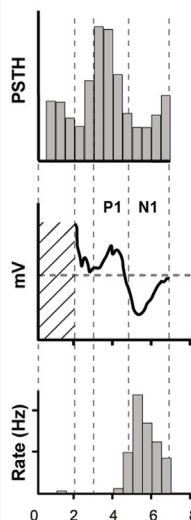
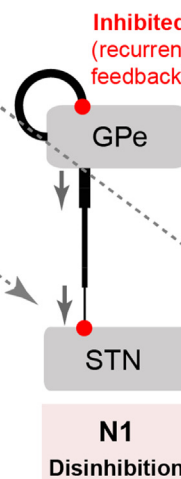
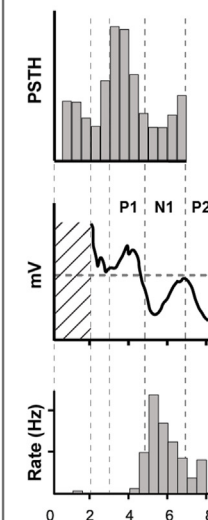
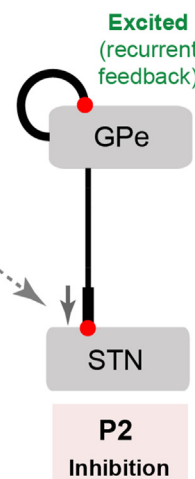
The complexity surrounding neural oscillators, and the unclear explanation of resonance phenomena in neural networks, have led different research groups to adopt varying terms to describe DBS-induced EPs (Table 1). Schmidt et al. [13] referred to these signals as a “DBS Local Evoked Potentials”, Realmuto et al [19] used the term “Evoked Oscillatory Neural Responses,” while others have opted for the more general terms “Evoked Compound Activity” and “Evoked Compound Action Potentials” [17,35]. Moving forward, we propose that the research community should simply adopt the ERNA acronym for consistency and clarity, while acknowledging a more general definition of “Evoked Recurrent Neural Activity”. We propose that this will streamline cross-referencing among studies on these especially interesting signals.

Dissecting ERNA in the STN

During the ~7.7 ms interval between two successive DBS pulses at 130 Hz, ERNA in the STN consists of two positive (P1 and P2) and one

Table 1  
Terminologies used to describe DBS evoked responses.

Paper	Term	Acronym	Keyword
Sinclair 2018	Evoked resonant neural activity	ERNA	Resonant
Schmidt 2020	DBS local evoked potentials	DLEPs	DBS, local
Ozturk 2021	Evoked compound activity	ECA	Compound
Awad 2021	Subcortical field potential/Subcortical evoked potential/Evoked resonant neural activity	ERNA	Subcortical
Wiest 2022	Evoked neural activity (response to a single DBS pulse), ERNA (response during or after a train of DBS pulses)	ENA/ERNA	
Rosing 2023	Evoked compound action potential	ECAP	Compound
Realmuto 2023	Evoked oscillatory neural activity	EONR	Oscillatory
Steiner 2023	Evoked resonant neural activity	ERNA	
Johnson 2023	Evoked resonant neural activity	ERNA	

**A. Subthalamo-pallidum Circuit****B. i. Afferent / efferent fibers activated****B. ii. 0.5 - 2 ms****iii. 2 - 3 ms****iv. 3 - 5 ms****v. 5 - 7 ms****vi. t > 7 ms**

Evoked firing in GPe (Hashimoto 2003)  
Evoked potential in STN (Steiner 2023)  
Evoked firing in STN (Steiner 2023)

**Fig. 2.** Sequence of events involved in STN ERNA generation. A) Subthalamo-pallidal microcircuit, from the perspective of the STN. STN receives inhibitory input from GPe and cortical excitatory input via the hyperdirect pathway. GPe receives excitatory input from STN and inhibitory feedback from other GPe neurons. B) Sequence of events after a DBS pulse. i) STN afferents and efferents are activated by the DBS pulse. ii) 0.5–2 ms, antidromic input excites GPe. iii) 2–3 ms, GPe recurrent feedback inhibits GPe. vi) 3–5 ms, orthodromic input from STN excites GPe again. In parallel, GPe input from step (ii) arrives at STN to help shape P1 in the STN field potential. (v) 5–7 ms, GPe recurrent feedback again inhibits GPe. In parallel, GPe input from step (iii) arrives at STN and causes disinhibition – manifested as N1 in the STN field potential. vi) After 7 ms, GPe input from step (iv) arrives at STN and again causes inhibition – manifested as P2 in the STN field potential.



negative peak (N1) (Fig. 1). P1 peaks at  $\sim 4$  ms, followed by N1 at  $\sim 5$  ms, and finally P2 at  $\sim 7$  ms [17,13,14,15]. To comprehend the origins of these EP waveform components, it is imperative to consider the afferent and efferent fibers connected to the STN [36], as well as the respective action potential (AP) conduction times and synaptic delays between the STN and pallidum (Fig. 2). Our analyses start with some major simplifying assumptions on the circuitry of cortico-subthalamo-pallidal network. Under this simplified model, the STN receives excitatory input from the cortex via the hyperdirect pathway and inhibitory input from the globus pallidus externus (GPe) via the pallido-subthalamic pathway. The GPe receives excitatory input from the STN via the subthalamo-pallidal pathway, along with reciprocal inhibitory input from other GPe neurons. The individual neurons of both the STN and GPe are intrinsically active with relatively high baseline rates of firing. Therefore, they can be affected by synaptic modulation, via either excitatory or inhibitory neurotransmitters, causing their activity to modulate around an average firing rate.

Each STN DBS pulse directly activates a range of different afferent and efferent fibers that surround the DBS electrode (Fig. 2B) [37,38]. In this review, we will concentrate on the effects associated with the simultaneous initiation of APs in three different neural populations at time zero. One neural population comprises of the STN projection neurons [39]. APs initiate in their axons [38], and travel in two directions: antidromically to the STN soma and orthodromically to invade their axon terminals in the globus pallidus. A second neural population is the globus pallidus afferent inputs to the STN [40]. APs initiate in their afferent axonal arbor [41], which also propagate in both directions: orthodromically throughout the arbor to their GABAergic synaptic terminals in the STN and antidromically back to the globus pallidus [42]. The third neural population is the hyperdirect afferent inputs from cortex to the STN [43]. APs initiate in their afferent axonal arbor and then propagate in both directions: orthodromically throughout the arbor to their glutamatergic synaptic terminals in the STN [44] and antidromically up to the cortex [45]. Therefore, one DBS pulse generates a wide array of APs in many different neurons that propagate in multiple directions and invade many different synaptic terminals throughout the cortico-subthalamo-pallidal network (Fig. 2).

DBS-induced activation of the hyperdirect pathway afferent inputs provides an excitatory synaptic drive to the STN neurons [44]. However, the simultaneous activation of the GPe afferent inputs produces a more potent inhibitory effect on the cell body signaling of STN neurons [23]. Therefore, during the initial time window following the DBS pulse (i.e.  $\sim 0.5$ – $2$  ms), the net effect on STN neuron cell body firing is most likely a general inhibition, albeit a mix of many competing synaptic currents [38, 46]. While this initial inhibition should manifest as a positive peak in the field potential recording, the details of the early waveform are typically obscured by the stimulation artifact (Fig. 2Bii). Nonetheless, the shape of the P1 STN field potential is most likely driven by the inhibitory GPe synaptic currents that were activated by the DBS pulse.

The early phase of the STN ERNA is created by the local interactions of neural elements near the DBS electrode. Moving forward in time requires accounting for the AP conduction delays between the STN and pallidum (i.e.  $\sim 1$  ms each way), as well as the synaptic transmission delays associated with AP arrival in the terminals and the subsequent generation of post-synaptic currents (i.e.  $\sim 2$  ms). Therefore, when spiking activity in one nucleus is elevated, there is a  $\sim 3$  ms lag to its subsequent action on the other nucleus.

DBS-induced activation of the GPe afferent inputs in the STN leads to an antidromic excitation of GPe neurons. These antidromic effects in GPe are seen at  $0.5$ – $2$  ms after the STN DBS pulse (Fig. 2Bii), subsequently inhibiting the STN from  $3$ – $5$  ms and resulting in the P1 STN field potential (Fig. 2Biv). As a result of the antidromic excitation of GPe neurons, other GPe neurons experience a suppression of their tonic firing during the  $2$ – $3$  ms time window because of their recurrent inhibitory synaptic connections onto each other (Fig. 2Biii). This effect acts to

### GPe ERNA during and after a train of pulses at 135 Hz GPi DBS

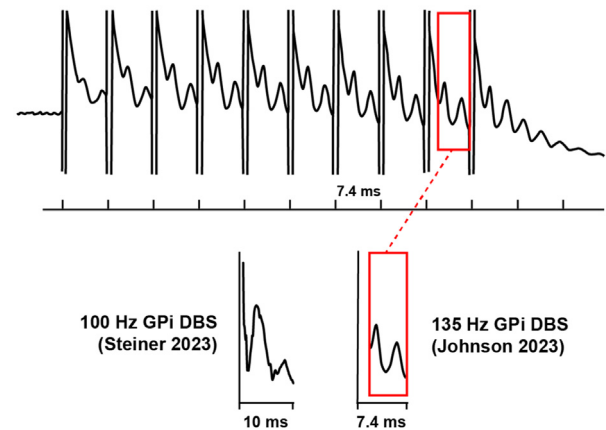


**Fig. 3.** GPe ERNA. Example signals elicited during and after a train of DBS pulses delivered to the GPi of a PD patient at 135 Hz (Modified from Ref. [12]. On the bottom left, GPi ERNA elicited during 100 Hz GPi DBS (Modified from Ref. [47].

briefly release the STN neurons from their pallidal inhibition, leading to the N1 STN field potential from  $4$  to  $6$  ms (Fig. 2Bv).

The DBS-induced orthodromic APs in the STN efferent axons arrive at the GPe and begin having an effect on GPe firing at  $\sim 3$  ms. These signals provide an excitatory synaptic drive to the GPe neurons, leading to increased GPe firing during the  $3$ – $5$  ms time window (Fig. 2Biv). As a result, the GPe provides the STN with robust inhibition, arriving in the  $5$ – $7$  ms time window (Fig. 2Bv). These inhibitory GPe inputs then create the P2 STN field potential from  $6$  to  $8$  ms (Fig. 2Bvi). Therefore, GPe recurrent inhibition and subsequent excitation leads to STN disinhibition at  $\sim 5$  ms (N1) and inhibition at  $\sim 7$  ms (P2), respectively.

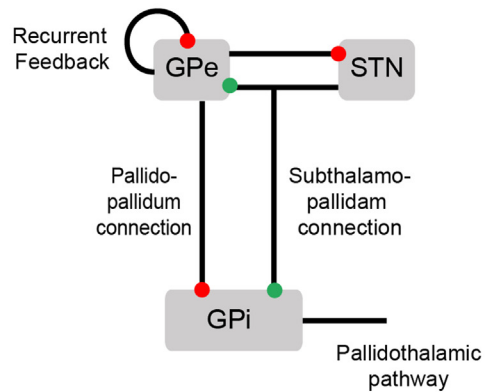
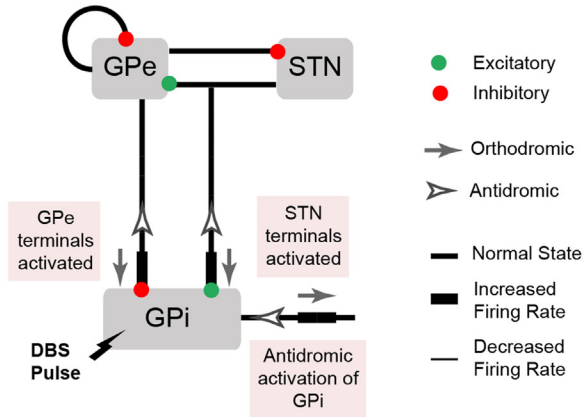
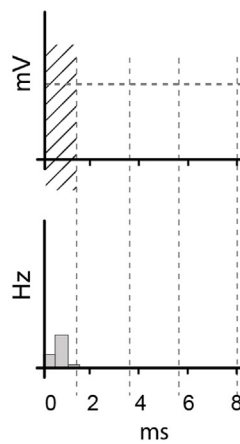
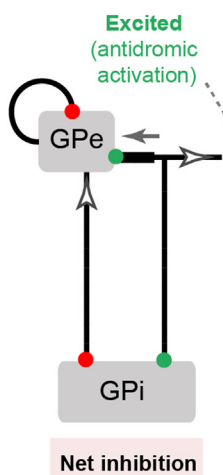
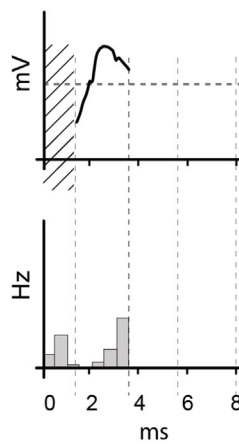
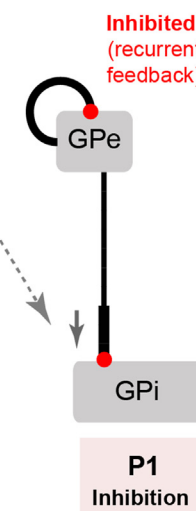
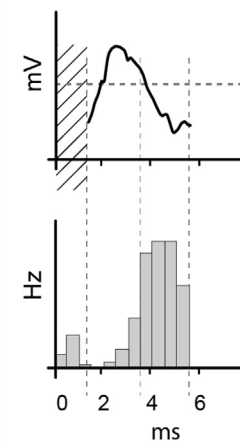
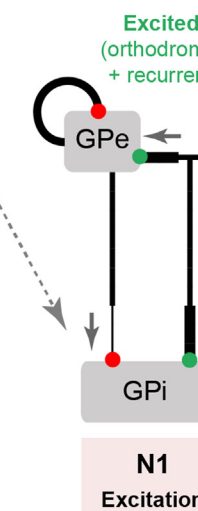
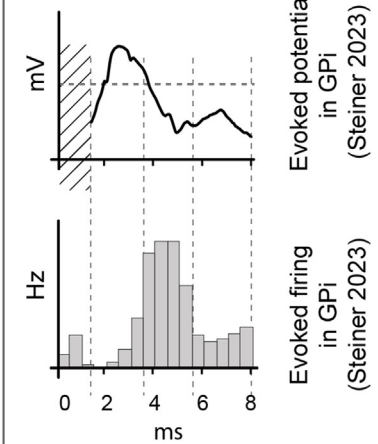
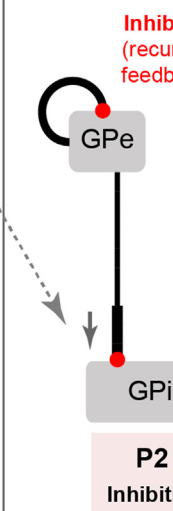
The cascade of events described above provides a general explanation of ERNA waveform creation, as observed in between  $130$  Hz DBS pulses. However, ERNA can also persist as a damped oscillation within the subthalamo-pallidal network if a DBS pulse is skipped or the stimulus train has ended (Fig. 1). Under these circumstances, we observe the natural push-pull (inhibitory-excitatory) of the STN interacting with the GPe, where cycle of their oscillation recurs. However, with each cycle the subthalamo-pallidal network becomes less synchronized overall, resulting in subsequently smaller field potentials, which eventually decay back to a baseline level.

### Dissecting ERNA in the GPi

As STN DBS generates ERNA in the STN, GPi DBS also evokes similar signals in the GPi. The most pronounced ERNAs have been observed in the postero-dorsal pallidum [12]. Much like STN ERNA, GPi ERNA appears to have relevance as an electrophysiological biomarker of therapeutic target engagement. The recent study of Johnson et al. [12] found that in  $70\%$  of tested hemispheres, the contact that generated the largest ERNA amplitude was also the clinically most effective contact for stimulation.

GPi ERNA exhibits two positive peaks (P1 and P2) and one negative peak (N1), which is analogous to STN ERNA (Fig. 3). In response to  $100$  Hz GPi DBS, P1 emerges at  $\sim 3$  ms, followed by N1 at  $\sim 5$  ms, and finally, P2 at  $\sim 6.5$  ms [47]. When using  $135$  Hz DBS, these latencies reduce by about  $1$  ms: P1 appears at  $\sim 2$  ms, N1 at  $\sim 4$  ms, and P2 at  $\sim 5.5$  ms [12].

Dissecting the network origin of the GPi ERNA signal components requires consideration of the afferent and efferent fiber connections to the GPi. Within the simplified subthalamo-pallidal network model, the GPi receives inhibitory input from GPe, excitatory input from STN, and sends inhibitory projections to the thalamus (Fig. 4A). Similar to STN DBS, GPi DBS directly activates both afferent and efferent fibers

**A. Subthalamo-pallidum Circuit****B. i. Afferent / efferent fibers activated****B. ii. 0.5 - 1.5 ms****iii. 1.5 - 3.5 ms****iv. 3.5 - 5.5 ms****v. 5.5 - 8 ms**

**Fig. 4.** Sequence of events involved in GPi ERN generation. A) Subthalamo-pallidal microcircuit, from the perspective of GPi. GPi receives inhibitory input from GPe and excitatory input from the STN. GPi also sends inhibitory projections to the thalamus. GPe receives excitatory input from STN and inhibitory feedback from other GPe neurons. B) Sequence of events after a DBS pulse. i) GPi afferent and efferent are activated by the DBS pulse. ii) 0.5–1.5 ms, antidromic input excites GPe. iii) 1.5–3.5 ms, GPe recurrent feedback inhibits the GPe. In parallel, the GPe output from step (ii) arrives at GPi and causes inhibition – manifested as P1 in the GPi LFP. vi) 3.5–5.5 ms, excitatory drive from the engaged STN drives both GPe and GPi. In parallel, the GPe output from step (iii) arrives at GPi and causes disinhibition – manifested as N1 in the GPi LFP. v) 5.5–8 ms, GPe output from step (iv) arrives at GPi and again causes inhibition – manifested as P2 in the GPi LFP.

surrounding the electrode (Fig. 4Bi) [48]. Activation of the subthalamo-pallidal terminals (STN afferent inputs) and the antidromic activation of the pallidothalamic fibers (GPI efferent outputs) have an excitatory effect on the GPI, while activation of the pallido-pallidal terminals (GPe afferent inputs) exert a stronger inhibitory effect. This results in a net inhibition of GPI cell body firing immediately after the DBS pulse (Fig. 4Bii). This inhibition would likely manifest as a positive peak in the LFP recording, but it is obscured by the stimulation artifact. In parallel with these effects on the GPI neurons, the antidromic activation of the pallido-pallidal fibers, as well as orthodromic activation of the subthalamo-pallidal fibers, enhances GPe firing around 0.5–1.5 ms after the stimulus pulse (Fig. 4Bii). This GPe excitation then works to inhibit the GPI around 1.5–3.5 ms, which is manifested as P1 in the GPI LFP (Fig. 4Biii). Recurrent inhibitory feedback from the GPe onto itself then acts to inhibit the GPe. In turn, the GPe releases the GPI from its inhibition around 3.5–5.5 ms. Approximately at the same time, excitation from the STN also arrives at the pallidum, resulting in an increase in both GPe and GPI activity. This excitation of the GPI is manifested as N1 in the GPI LFP (Fig. 4Biv). Finally, GPe excitation once again inhibits the GPI around 5.5–8 ms, which is reflected as P2 in the GPI LFP.

Interestingly, GPI DBS has also been shown to produce ERNA in the STN [49]. Vitek et al. [50] also observed a similar cycle of inhibition, disinhibition, and inhibition in the GPI with similar latencies when stimulating the GPe of non-human primates. Therefore, it appears that ERNA is a basic feature of the subthalamo-pallidal system and it can be engaged by stimulating any part of the system.

### STN vs GPI Evoked Neural Activity

The amplitude of the GPI ERNA induced by GPI DBS is notably smaller than the STN ERNA induced by STN DBS [12]. One possible explanation for the reduced amplitude of GPI ERNA is its close proximity to the GPe, where neural activity often opposes that of the GPI (i.e. excitation in the GPe leads to inhibition in the GPI, and vice versa). This likely keeps the field potentials in the two nuclei out of phase, thereby limiting their recording amplitudes relative to what can be seen in the STN. In addition, the width of P1 as recorded in GPI is broader than the P1 seen in STN. This indicates a greater temporal distribution of the synaptic inputs, which would translate into a smaller ERNA amplitude. Nonetheless, the pallidal EP signals are still substantially larger (i.e. mV) than intrinsic neural activity (i.e.  $\mu$ V) patterns, which makes them attractive candidates as electrophysiological biomarkers of DBS target engagement [12].

### Limitations and Future Directions

In this review, we investigated the roles of different neural populations in the genesis of ERNA. However, our interpretations are limited by the use of a simplified model of the subthalamo-pallidal network. Both the STN and pallidum have connections to other brain regions, such as the pedunculopontine nucleus [51], and more detailed models of the basal ganglia have been proposed [52]. Therefore, future studies incorporating more advanced representations of the network structure may offer a more comprehensive understanding of the mechanisms underlying ERNA. In addition, the exacting details of AP signal conduction times and post-synaptic potential time courses are likely play important roles in dissecting the details of ERNA waveforms.

As ERNA research progresses, we propose that key next steps in the analyses should focus on simultaneous recordings from multiple basal ganglia nuclei during subthalamic or pallidal DBS. Such recordings, could enhance our understanding of the signaling details between the different neural populations and how they contribute to ERNA generation. Additionally, conducting a comparative analysis of GPI ERNA resulting from pallidal DBS in patients with either Parkinson's disease or dystonia could provide novel insights on the neural mechanisms underlying those different movement disorders.

DBS-induced EPs in the basal ganglia are a robust phenomenon that emerge by activating oscillations within the subthalamo-pallidal network. This prototypical excitatory-inhibitory microcircuit is easily pushed into action by the strong synchronous activation of its neural components by DBS. Our analyses of the available data suggest that DBS-induced antidromic activation of GPe is a key driver of these oscillatory EPs, independent of stimulation location (i.e. STN or GPI). This highlights a potential relevance of the GPe in the mechanisms of DBS, which has also been noted in previous computational [48] and optogenetic [53] analyses. In addition, ERNA signals have potential to become useful electrophysiological biomarkers for verification of DBS target engagement. These biomarkers can be elicited in either awake or asleep DBS surgeries, and the continued monitoring of ERNA engagement over time could represent an alternative to beta-band LFP signals for use in closed-loop DBS systems.

### Author's Contributions

Conceptualization: MSN, CCM; Methodology: MSN, AKS, CCM; Formal analysis and investigation: MSN, AKS; Writing: MSN, CCM; Funding acquisition: CCM.

### Funding

This work was supported by a grant from the National Institutes of Health (NIH R01 NS119520).

### Declaration of competing interest

CCM is a paid consultant for Boston Scientific Neuromodulation, receives royalties from Hologram Consultants, Neuros Medical, Qr8 Health, Ceraxis Health, and is a shareholder in the following companies: Hologram Consultants, Surgical Information Sciences, BrainDynamics, CerGate, Cardionomic, Enspire DBS.

### References

- [1] Obeso JA, Olanow CW, Rodriguez-Oroz MC, Krack P, Kumar R, Lang AE. Deep-brain stimulation of the subthalamic nucleus or the pars interna of the globus pallidus in Parkinson's disease. *N Engl J Med* 2001;345(13):956–63.
- [2] Hamel W, Koppen JA, Alesch F, Antonini A, Barcia JA, Bergman H, et al. Targeting of the subthalamic nucleus for deep brain stimulation: a survey among Parkinson disease specialists. *World Neurosurg* 2017;99:41–46.
- [3] McClelland S, Ford B, Senatus PB, Winfield LM, Du YE, Pullman SL, et al. Subthalamic stimulation for Parkinson disease: determination of electrode location necessary for clinical efficacy. *Neurosurg Focus* 2005;19(5):E12.
- [4] Vitek JL, Patriat R, Ingham L, Reich MM, Volkmann J, Harel N. Lead location as a determinant of motor benefit in subthalamic nucleus deep brain stimulation for Parkinson's disease. *Front Neurosci* 2022;16:1010253.
- [5] Campbell BA, Machado AG, Baker KB. Electrophysiologic mapping for deep brain stimulation for movement disorders. *Handb Clin Neurol* 2019;160:345–355.
- [6] Hammond C, Bergman H, Brown P. Pathological synchronization in Parkinson's disease: networks, models and treatments. *Trends Neurosci* 2007;30(7):357–64.
- [7] Kühn AA, Tsui A, Aziz T, Ray N, Brucke C, Kupsch A, et al. Pathological synchronisation in the subthalamic nucleus of patients with Parkinson's disease relates to both bradykinesia and rigidity. *Exp Neurol* 2009;215(2):380–7.
- [8] Little S, Pogossyan A, Neal S, Zavala B, Zrinzo L, Hariz M, Brown P. Adaptive deep brain stimulation in advanced Parkinson disease. *Ann Neurol* 2013;74(3):449–57.
- [9] Ho AL, Ali R, Connolly ID, Henderson JM, Dhali R, Stein SC, et al. Awake versus asleep deep brain stimulation for Parkinson's disease: a critical comparison and meta-analysis. *J Neurol Neurosurg Psychiatry* 2018;89(7):687–91.
- [10] Hölleijn RA, Verbaan D, van den Munckhof PM, Bot M, Geurtsen GJ, Dijk JM, et al. General anesthesia vs local anesthesia in microelectrode recording-guided deep-brain stimulation for Parkinson disease: the GALAXY randomized clinical trial. *JAMA Neurol* 2021;78(10):1212–9.
- [11] Bos MJ, Buhre W, Temel Y, Joosten EAJ, Absalom AR, Janssen MLF. Effect of anesthesia on microelectrode recordings during deep brain stimulation surgery: a narrative review. *J Neurosurg Anesthesiol* 2021;33(4):300–7.
- [12] Johnson KA, Cagle JN, Lopes JL, Wong JK, Okun MS, Gunduz A, et al. Globus pallidus internus deep brain stimulation evokes resonant neural activity in Parkinson's disease. *Brain Commun* 2023;5(2):fcd025.
- [13] Schmidt SL, Brocker DT, Swan BD, Turner DA, Grill WM. Evoked potentials reveal neural circuits engaged by human deep brain stimulation. *Brain Stimul* 2020;13(6):1706–18.

- [14] Sinclair NC, McDermott HJ, Bulluss KJ, Fallon JB, Perera T, Xu SS, Thevathasan W. Subthalamic nucleus deep brain stimulation evokes resonant neural activity. *Ann Neurol* 2018;83(5):1027–31.
- [15] Wiest C, He S, Duchet B, Pogossyan A, Benjaber M, Denison T, Tan H. Evoked resonant neural activity in subthalamic local field potentials reflects basal ganglia network dynamics. *Neurobiol Dis* 2023;178:106019.
- [16] Sinclair NC, McDermott HJ, Fallon JB, Perera T, Brown P, Bulluss KJ, et al. Deep brain stimulation for Parkinson's disease modulates high-frequency evoked and spontaneous neural activity. *Neurobiol Dis* 2019;130:104522.
- [17] Ozturk M, Viswanathan A, Sheth SA, Ince NF. Electroceutically induced subthalamic high-frequency oscillations and evoked compound activity may explain the mechanism of therapeutic stimulation in Parkinson's disease. *Commun Biol* 2021;4(1):393.
- [18] Sinclair NC, Fallon JB, Bulluss KJ, Thevathasan W, McDermott HJ. On the neural basis of deep brain stimulation evoked resonant activity. *Biomedical Physics & Engineering Express* 2019;5:057001.
- [19] Realmuto J, Vidmark J, Sanger T. Modeling deep brain stimulation evoked responses with phase oscillator networks. In: 11th international IEEE/EMBS conference on neural engineering (NER); 2023. p. 1–4.
- [20] Wiest C, Torrecillos F, Tinkhauser G, Pogossyan A, Morgante F, Pereira EA, et al. Finely-tuned gamma oscillations: spectral characteristics and links to dyskinesia. *Exp Neurol* 2022;351:113999.
- [21] Sinclair NC, McDermott HJ, Lee WL, Xu SS, Acevedo N, Begg A, Bulluss KJ. Electrically evoked and spontaneous neural activity in the subthalamic nucleus under general anesthesia. *J Neurosurg* 2021;132(2):449–58.
- [22] Dale J, Schmidt SL, Mitchell K, Turner DA, Grill WM. Evoked potentials generated by deep brain stimulation for Parkinson's disease. *Brain Stimul* 2022;15(5):1040–7.
- [23] Lempka SF, McIntyre CC. Theoretical analysis of the local field potential in deep brain stimulation applications. *PLoS One* 2013;8(3):e59839.
- [24] Buzsáki G, Anastassiou CA, Koch C. The origin of extracellular fields and currents—EEG, ECoG, LFP and spikes. *Nat Rev Neurosci* 2012;13(6):407–20.
- [25] Bazelot M, Dinocourt C, Cohen I, Miles R. Unitary inhibitory field potentials in the ca3 region of rat hippocampus. *J Physiol* 2010;588(Pt 12):2077–90.
- [26] Brunner H, Misgeld U. Synaptic activation in Guinea-pig dentate area: dependence on the stimulation site. *Pflügers Archiv* 1993;423:497–503.
- [27] Shewcraft RA, Dean HL, Fabiszak MM, Hagan MA, Wong YT, Pesaran B. Excitatory/inhibitory responses shape coherent neuronal dynamics driven by optogenetic stimulation in the primate brain. *J Neurosci* 2020;40(10):2056–68.
- [28] Bruyns-Haylett M, Luo J, Kennerley AJ, Harris S, Boorman L, Milne E, et al. The neurogenesis of P1 and N1: a concurrent EEG/LFP study. *Neuroimage* 2017;146: 575–88.
- [29] Yin Z, Zhu G, Zhao B, Bai Y, Jiang Y, Neumann WJ, et al. Local field potentials in Parkinson's disease: a frequency-based review. *Neurobiol Dis* 2021;155: 105372.
- [30] Awad MZ, Vaden RJ, Irwin ZT, Gonzalez CL, Black S, Nakhmani A, Walker HC. Subcortical short-term plasticity elicited by deep brain stimulation. *Ann Clin Transl Neurol* 2021;8(5):1010–23.
- [31] Muller M, Goutman JD, Kochubey O, Schneggenburger R. Interaction between facilitation and depression at a large CNS synapse reveals mechanisms of short-term plasticity. *J Neurosci* 2010;30(6):2007–16.
- [32] Wiest C, Tinkhauser G, Pogossyan A, Bange M, Muthuraman M, Groppa S, et al. Local field potential activity dynamics in response to deep brain stimulation of the subthalamic nucleus in parkinson's disease. *Neurobiol Dis*. 2020;143:105019.
- [33] Malagarriga D, Garcia-Vellica MA, Villa AE, Buldu JM, Garcia-Ojalvo J, Pons AJ. Synchronization-based computation through networks of coupled oscillators. *Front Comput Neurosci* 2015;9:97.
- [34] Doelling KB, Assaneo MF. Neural oscillations are a start toward understanding brain activity rather than the end. *PLoS Biol* 2021;19(5):e3001234.
- [35] Rosing J, Doyle A, Brinda A, Blumenfeld M, Lecy E, Spencer C, Johnson MD. Classification of electrically-evoked potentials in the parkinsonian subthalamic nucleus region. *Sci Rep* 2023;13(1):2685.
- [36] Parent M, Parent A. The microcircuitry of primate subthalamic nucleus. *Parkinsonism Relat Disorders* 2007;13(Suppl 3):S292–5.
- [37] Bower KL, Noecker AM, Frankemolle-Gilbert AM, McIntyre CC. Model-Based analysis of pathway recruitment during subthalamic deep brain stimulation. *Neuromodulation* 2024;27(3):455–63.
- [38] Miocinovic S, Parent M, Butson CR, Hahn PJ, Russo GS, Vitek JL, et al. Computational analysis of subthalamic nucleus and lenticular fasciculus activation during therapeutic deep brain stimulation. *J Neurophysiol* 2006;96(3):1569–80.
- [39] Sato F, Parent M, Levesque M, Parent A. Axonal branching pattern of neurons of the subthalamic nucleus in primates. *J Comp Neurol* 2000;424(1):142–52.
- [40] Sato F, Lavallée P, Lévesque M, Parent A. Single-axon tracing study of neurons of the external segment of the globus pallidus in primate. *J Comp Neurol* 2000;417(1): 17–31.
- [41] Bower KL, McIntyre CC. Deep brain stimulation of terminating axons. *Brain Stimul* 2020;13(6):1863–70.
- [42] Grill WM, Cantrell MB, Robertson MS. Antidromic propagation of action potentials in branched axons: implications for the mechanisms of action of deep brain stimulation. *J Comput Neurosci* 2008;24(1):81–93.
- [43] Coudé D, Parent A, Parent M. Single-axon tracing of the corticosubthalamic hyperdirect pathway in primates. *Brain Struct Funct* 2018;223(9):3959–73.
- [44] Bingham CS, McIntyre CC. Subthalamic deep brain stimulation of an anatomically detailed model of the human hyperdirect pathway. *J Neurophysiol* 2022;127(5): 1209–20.
- [45] Anderson RW, Farokhniaee A, Gunalan K, Howell B, McIntyre CC. Action potential initiation, propagation, and cortical invasion in the hyperdirect pathway during subthalamic deep brain stimulation. *Brain Stimul* 2018;11(5):1140–50.
- [46] Hashimoto T, Elder CM, Okun MS, Patrick SK, Vitek JL. Stimulation of the subthalamic nucleus changes the firing pattern of pallidal neurons. *J Neurosci* 2003; 23(5):1916–23.
- [47] Steiner LA, Milosevic L. A convergent subcortical signature to explain the common efficacy of subthalamic and pallidal deep brain stimulation. *Brain Commun* 2023; 5(2):fcad033.
- [48] Johnson MD, McIntyre CC. Quantifying the neural elements activated and inhibited by globus pallidus deep brain stimulation. *J Neurophysiol* 2008;100(5):2549–63.
- [49] Schmidt SL, Dale J, Turner DA, Grill WM. Simultaneous DBS local evoked potentials in the subthalamic nucleus and globus pallidus during local and remote deep brain stimulation. *Brain Stimul* 2023;16(1):352–3.
- [50] Vitek JL, Zhang J, Hashimoto T, Russo GS, Baker KB. External pallidal stimulation improves parkinsonian motor signs and modulates neuronal activity throughout the basal ganglia thalamic network. *Exp Neurol* 2012;233(1):581–6.
- [51] Muthusamy KA, Aravamuthan BR, Kringelbach ML, Jenkinson N, Voets NL, Johansen-Berg H, et al. Connectivity of the human pedunculopontine nucleus region and diffusion tensor imaging in surgical targeting. *J Neurosurg* 2007;107(4): 814–20.
- [52] Nelson AB, Kreitzer AC. Reassessing models of basal ganglia function and dysfunction. *Annu Rev Neurosci* 2014;37(1):117–35.
- [53] Spix TA, Nanivadekar S, Toong N, Kaplow IM, Issett BR, Goksen Y, Gittis AH. Population-specific neuromodulation prolongs therapeutic benefits of deep brain stimulation. *Science* 2021;374(6564):201–6.